Available at www.sciencedirect.com

ScienceDirect

journal homepage: www.elsevier.com/locate/he

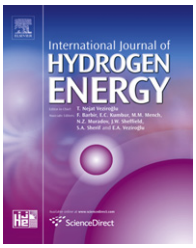

Hysteresis behavior of electrical resistance in Pd thin films during the process of absorption and desorption of hydrogen gas

Eunsongyi Lee [a,1], *Jun Min Lee* [a,1], *Ja Hoon Koo* [b], *Wooyoung Lee* [a,*], *Taeyoon Lee* [b,**]

[a] *Department of Materials Science and Engineering, Yonsei University, Seoul 120-749, Republic of Korea*
[b] *Nanobio Device Laboratory, School of Electrical and Electronic Engineering, Yonsei University, Seoul 120-749, Republic of Korea*

ARTICLE INFO

Article history:
Received 18 February 2010
Received in revised form
11 April 2010
Accepted 11 April 2010
Available online 23 May 2010

Keywords:
Palladium
Hydrogen
Sensor
Resistance
Hysteresis
Absorption
Desorption
Deformation

ABSTRACT

We report the fabrication of a novel hydrogen sensor that utilizes the electrical resistance changes in the palladium thin films with nanometer thicknesses. The sensing mechanism is based on transitory absorption of hydrogen atoms into the palladium layer, which leads to the reversible alteration of the electrical resistance. In concentrated hydrogen ambient, the excess hydrogen absorption process leads to mechanical deformation on the surface of the palladium films, corresponding to the phase transition from α-phase to β-phase. The reversible sensing process results in a hysteresis curve for resistive properties, of which the height (sensitivity) could be controlled by manipulating the thickness of the palladium layers. The peel-off phenomena on the surface of the palladium film were suppressed by decreasing the thickness of the film. At the thickness of 20 nm, a hysteresis curve of resistance was obtained without any structural change in the palladium thin film. These results provide a significant insight to the fundamental understanding of the relationship between the electrical sensitivity of pure Pd thin films and related structural deformation, which is essential to develop robust H-sensors with high sensibility.

1. Introduction

Hydrogen (H) is a promising alternative resource for generating green energy [1–3], however, a high performance sensing system is required for its handling to alleviate safety issues due to its explosive nature [4]. For this reason, extensive researches have been conducted to explore efficient H sensible devices with various material systems such as palladium (Pd) [5–7], indium oxide-doped tin oxide [8], titanium oxide nanotubes [9], and zirconia [10]. In particular, Pd–H systems are popular experimental subjects due to their broad applicability in H-storing devices, hydrogenation catalysts, and H_2 sensors [11,12]. Specifically, sensors using Pd thin layers that detect H in air by measuring the electrical properties are highly beneficial owing to their compatibility with conventional integrated circuits. Among such sensors, the resistive-type sensor built on the Pd system [13,14], which measures the changes in resistivity of the thin Pd films due to the absorption of H atoms, has received great attentions since its selectivity to H is greater than the hot wire type [15] and its comparable convenience in the manufacturing process compared to that of the metal-oxide-semiconductor (MOS) type sensors [16,17].

* *Corresponding author*. Tel.: +82 2 21232834; fax: +82 2 312 5375.
** *Corresponding author*. Tel.: +82 2 21237453; fax: +82 2 313 2879.
E-mail addresses: wooyoung@yonsei.ac.kr (W. Lee), taeyoon.lee@yonsei.ac.kr (T. Lee).
[1] These authors equally contributed to this work.

0360-3199/$ – see front matter © 2010 Professor T. Nejat Veziroglu. Published by Elsevier Ltd. All rights reserved.
doi:10.1016/j.ijhydene.2010.04.051

Lewis et al. [12] investigated the fundamental mechanism of the hydrogen absorption and desorption process in the Pd thin film using a pressure-composition isotherm. The linear increase in the electrical resistance of the Pd–H system as a function of H content has been successfully revealed. However, the results were obtained using the electrolytic charging method, and thus all the data acquisition was carried out in an environment at much higher pressure than atmospheric pressure. Although the gas phase method was introduced to compensate for the high-pressure-experimental-environment of the electrolytic charging method [18], Pd samples were still exposed to hydrogen gas (H_2) at higher pressure than the atmospheric level of up to 3.3 MPa [18,19]. Hence, various studies have been conducted to develop practical devices that work at atmospheric pressure, and it has not been over a few years that the H-sensors using thin Pd films were developed to work at the required environment [20,21].

In the Pd–H system, two phases of α-phase (solid solution of Pd and H) and β-phase (Pd hydride) can be obtained according to the amount of H atom incorporation into the thin Pd films [12]. A phase transition from the α- to β-phase occurs during the absorption process of H atoms if the amount of incorporated H atoms exceeds the maximum H solid solubility in the Pd layer [11,12,22]. During the course of the phase transition from the α- to β-phase and back to the α-phase, a hysteretic behavior in the resistance [12,23] with irreversible structural changes [24–27] in the Pd films were observed. The structural changes in the Pd films could lead to severe stability problems; to solve the related concerns, many investigations were conducted to suppress the mechanical deformations. As a consequence, diverse methods were invented including the use of Pd alloys [28,29], addition of a buffer layer [20,21], and modifications of substrates such as crystallinity, surface morphologies, and thicknesses [25,30–34]. However, a fundamental understanding of the relationship between the structural deformation and sensitivity of pure thin Pd films, which can be the key to develop robust H-sensors with high sensibility, is lacking.

In this article, we report the effects of film thickness and concentrations of H_2 on the hysteretic characteristics of resistance and related mechanical deformations for pure thin Pd layers in the presence of H_2 at atmospheric ambient. The height of the hysteretic resistance curve, a measure of the H sensitivity of the Pd layer, increased as the thickness of the Pd films increased. For Pd films with thicknesses less than 5 nm, the hysteretic behavior in the resistance curve was no longer observed. On the other hand, the structural deformation of the Pd film was successfully repressed at thicknesses less than 20 nm. The presented experimental data is in accordance with the changes of the resistance predicted by the Sieverts' law in dilute hydrogen concentrations. The primary cause of the increase in the resistance of the Pd films can be attributed to the scattering by the incorporated H atoms in the interstitial states of the Pd–H system.

2. Experimental procedures

2.1. Device fabrications

Various nanometer-thick Pd films, ranging from 5 to 400 nm, were deposited on thermally oxidized 12.5 mm × 12.5 mm Si (100) substrates through sputter deposition using an ultra high-vacuum DC magnetron sputtering system with a base pressure of 4×10^{-8} Torr. The thickness of the oxide layer of the substrate was 300 nm. The substrates were cleaned and degreased with successive rinses in ultrasonic baths of acetone, methanol, and de-ionized water for 15 min each at room temperature. Then, the substrates were blown dry with nitrogen gas (N_2). The sample introduction chamber was vented with N_2 gas prior to sample transfer. Sputtering with 99.99% purity Pd target was performed in a 1.2×10^{-3} Torr discharge composed of 14 sccm argon gas injected into the deposition chamber. The discharge power was fixed at 20 W. The target-to-substrate separation was approximately 15 cm, resulting in a film deposition rate of 2.7 nm s^{-1}.

2.2. Sensing measurements

Electrical resistance measurements were collected using a four-point probe technique. The surfaces of the Pd thin films were connected by Au wires to a printed circuit board mounted in a test chamber with a volume capacity of ~250 mL. The test chamber was connected to a Ketheley 236 power supply and Ketheley 2182 digital multimeter to provide a constant current of 1 mA. The chamber was also equipped with a mass flow controller (MFC) that monitored the inflow/outflow ratio of H_2 and N_2, and the real-time electrical resistance response to H_2 was measured at room temperature. All data acquisitions were carried out with National Instruments LabView program through a General Purpose Interface Bus (GPIB) interface card. The test chamber had inlet and outlet lines for the flow of different gases. A check valve was set up at the outlet line to maintain the outflow of the gases in a single direction. To constantly maintain a near atmospheric pressure, the check valve opened when the pressure inside of the chamber was greater than the environmental pressure. The concentration of H_2 was controlled by its relative amount in mixture with N_2.

3. Results and discussion

Fig. 1(a) shows the representative electrical resistance (R) responses to the presence of 1% H_2 of the Pd thin film with a thickness $t = 100$ nm at room temperature. The measured value of R in an initial H_2-free environment was 0.469 Ω, followed by a substantial increase to 0.494 Ω after the H_2 exposure. When the chamber environment was changed to 100% N_2 ambient, as indicated with an arrow, the value of R rapidly decayed (within the first 50 s) and saturated to the value of the initial stage (base line). For repeatedly altering the exposure environment from 1% H_2 to 100% N_2, identical behaviors in the variation of R and corresponding sensitivity were observed. Here, the sensitivity S refers to the relative change between the R measured after the exposure to H_2 and the initial R of the Pd film. The sensitivity shown in the right axis of Fig. 1(a) was calculated by the following equation:

$$S = \frac{\Delta R}{R} \times 100(\%) = \frac{R_{H_2} - R_{N_2}}{R_{N_2}} \times 100(\%), \quad (1)$$

where R_{H_2} and R_{N_2} are the resistances of the Pd film in the presence of H_2 and N_2, respectively. The reversible periodicity

of R and corresponding sensitivity of Pd thin films can be explained by the following process. When the Pd thin film is exposed to H_2, the H_2 molecules are decomposed into single H atoms and they are absorbed in the interstitial sites of the Pd lattice through diffusion process as schematically described later in Fig. 2(a) and (b). The increment of R can be attributed to carrier scattering resulting from the incorporated H atoms in the Pd layer [22]. On the contrary, by replacing 1:99/H_2:N_2 with 100% N_2 ambient, the desorption of H atoms owing to the decrement in the partial pressure of H_2 occurred, resulting in the reduction of the resistivity of Pd film to the initial value.

The response time (T_{90}), which is the time to reach 90% of the total change in the R of the Pd film at a given concentration of H_2, was approximately 130 s in 1% H_2 ambient, demonstrating an excellent response time with lower concentrations of H_2 when compared to thin film sensors built with alternative materials [35,36]. Sensors fabricated with tungsten oxide thin films (in 7000 ppm CH_4 ambient) showed similar response time of 180 s [35]. A much slower sensing mechanism that required approximately 700 s of T_{90} was reported for the use of zinc oxide thin films (in 3% H_2 ambient) [36]. However, a noticeable reduction in the response time was discovered when using Pd nanocluster films (in 2% H_2 ambient) [14]: T_{90} of 70 ms was obtained. It can be attributed to the significantly larger effective exposed surface area of Pd nanocluster films compared to that of the Pd thin layer. Furthermore, a comparable response time of 150 s with much higher sensibility was

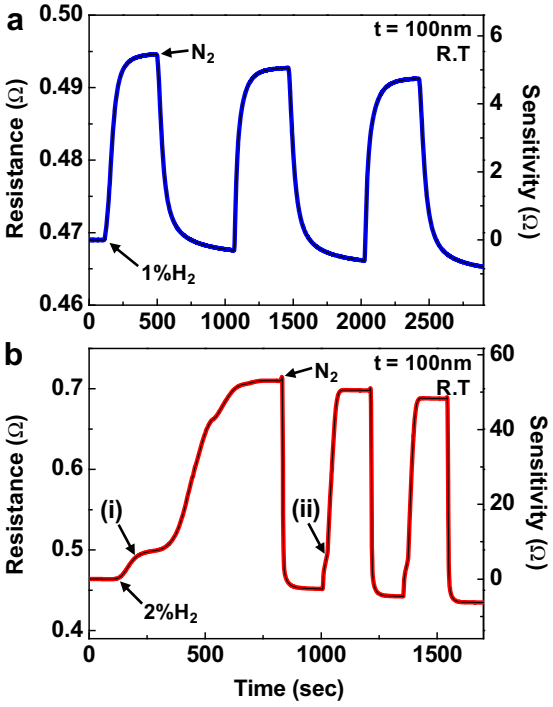

Fig. 1 – Electrical resistance responses and the corresponding sensitivity changes of the Pd thin film with a thickness of 100 nm to the presence of (a) 1% H_2 and (b) 2% H_2 at room temperature. The measurements were carried out while repeatedly varying the exposure environment to concentrated H_2 and pure N_2 back and forth.

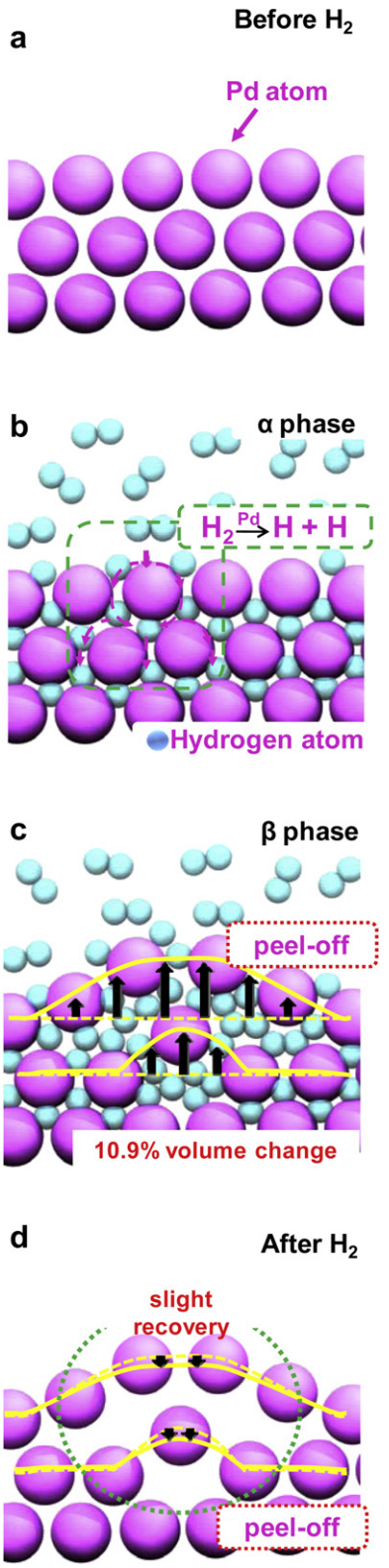

Fig. 2 – The sequential schematics of the Pd–H system during the phase transition from α- to β-phase by the sample exposure to concentrated H_2: (a) before H_2 introduction, (b) sample exposure to 1% H_2, (c) sample exposure to 2% H_2, and (d) after desorption process of H_2 by changing to pure N_2 ambient.

reported for the use of titania nanotubes (in 1000 ppm H_2 ambient) owing to the nature of its nano structure [37].

Fig. 1(b) remarks slightly dissimilar features for the resistance response curve under the same experimental procedures with 2% H_2. A two-step behavior was observed during the increase of R in the first cycle of the graph, and T_{90} was attained much later (approximately 480 s) compared to that of the sample exposed to 1% H_2. During the increment of R in the first cycle, an intermediate stage shown as a flat curve (indicated with (i)) was observed from approximately 250–375 s, followed by a further increase. It can be ascribed to the phase transition of the Pd thin film from the α- to β-phase. The maximum values obtained for R, and hence S, were 0.706 Ω and 52%, respectively, and the value of S was nearly ten times greater than that of the sample exposed to 1% H_2 ambient. After experiencing the two-step behavior, repeating the experiment with alternating the environment from 2:98/H_2:N_2 to 100% N_2 ambient produced a similar periodic pulse train of the change in R.

The increase in R for the Pd thin film exposed to 2% H_2 is most probably due to the carrier scattering owing to the excess amount of incorporated H atoms and additional defects such as vacancies and dislocations formed during the delamination process (shown later in Fig. 3) of the Pd surface. The delamination of the Pd thin film, which occurs during the phase transition from the α- to β-phase, is primarily the consequence of large amounts of H atoms diffusing into the film, where significant amounts of H atoms break the bonds of the Pd system, becoming detached. At the first point of inflection (indicated with (i)), the measured value of S was approximately 7.6%, which is greater than the overall values of S obtained in the experiment with 1% H_2. The α-phase of the Pd–H binary compound shows the maximum solid solubility of H atoms up to this point, and a dramatic increase in the resistance was followed along with the transition to the β-phase. During the desorption process of H atoms caused by changing the environment to pure N_2 ambient, a radical decrease in R (as well as in S) was achieved. For further alteration of the exposure environment, the shoulders (indicated as (ii)) in the increasing curve of R was barely shown (hence negligible), indicating that the deformed structure of the Pd film remained. Accordingly, T_{90} from the second periodic pulse train was significantly shortened to approximately 100 s. Using an *in-situ* optical microscope, the initial structural changes corresponding to the deformation of Pd film were observed from the first inflection point during the exposure to 2% H_2. The surface of the Pd film began to detach by forming small circular patterns and then these patterns expanded in an isotropic manner throughout the whole film (not shown). After the structural deformation process was finalized, the values of R and S were saturated accordingly.

Fig. 2 illustrates the full courses of the phase transition of the Pd thin film from the α- to β-phase during the exposure to H_2. Before the introduction of H_2, the crystalline structure of the Pd film is well organized, and Pd atoms are in the form of a robust lattice structure (Fig. 2(a)). However, when the film is exposed to H_2 ambient, the H_2 molecules diffuse into the surface of the Pd film, and break into single H atoms that are placed in between the Pd atoms due to the high reactivity of Pd atoms to H atoms (Fig. 2(b)). This state of the Pd film where the H atoms are interstitially placed in between the Pd atoms is defined as the α-phase, which can be found during the exposure of the Pd film to 1% H_2 (throughout the entire process), and exposure to 2% H_2 before the phase transition to β-phase initiates as depicted in Fig. 1(b).

For Pd films exposed to 2% H_2, further incorporation of H atoms into the Pd–H system induces a phase transition from the α- to β-phase. As the nucleation and growth of the β-phase arise out of the α-phase, an incoherent state can be induced to release the stress caused by the difference of the lattice constant between the α- and β-phases. The Pd layers tend to expand due to its volume increase during the phase transition, leading to a compressive stress at the interface of the film/substrate. To relieve the applied stress, mechanical deformation corresponding to a slight detachment of the Pd film is generated (Fig. 2(c)) [24–26]. The structural change in the Pd film is irreversible, and therefore, even after the H atoms are desorbed and removed from the system by decreasing the partial pressure of H_2, the deformed structure remains unchanged with only a slight recovery in shape (Fig. 2(d)).

Fig. 3 shows the representative scanning laser confocal images of the surfaces of the thin Pd films with different thicknesses of (a) 100 nm, (c) 50 nm, (e) 30 nm, and (g) 20 nm after exposure to 2% H_2. Fig. 3(b), (d), (f) and (h) are the magnified images of (a), (c), (e), and (g), respectively. For the Pd film with a thickness of 100 nm, large blisters in the shape of a mountain contour map with serious wrinkles are shown (Fig. 3(a) and (b)). The size of the blister was approximately 300–500 μm, and the blisters are observed throughout the entire surface of the Pd film. When the thickness of the film is decreased to 50 nm, a noticeable reduction in the size of the deformed regions can be observed, and the buckles are shaped more like telephone cores or wrinkles on a cloth (Fig. 3(c) and (d)). An additional decrease in the size and shape of the deformations is observed in the Pd film with a thickness of 30 nm, where the deformed structures are shown to be composed of small dots with rectangular or triangular shapes and patterned lines (Fig. 3(e) and (f)). When the thickness of the Pd film is less than 20 nm (Fig. 3(g) and (h)), no mechanical deformation is observed, which can be explained by the clamping effect, which states that the tensile stiffness of a laminate specimen is in an inverse relation to the thickness of the specimen [17]. Hence, the clamping effect played a major role in restraining the tensile strength induced in the Pd layer as the Pd layers were thinner. An interesting phenomenon to be noted is that even without the structural change of the thin Pd films, hysteretic behavior of S was observed according to the variation of H_2 concentration, which will be shown later in Fig. 4(b) for the 20 nm-thick Pd film.

To better understand the effect of H_2 concentration on the changes of R (as well as S) during the process of absorption and desorption of H, the exposure of H_2 was gradually increased and decreased between 0 and 2% for the Pd thin film with thicknesses of 100 nm and the corresponding experimental observations were plotted. As shown in Fig. 4(a), S followed a different curve in the absorption and desorption process. Two abrupt changes in S were observed: a sharp increase at 1.5% H_2 in the absorption process and a drastic decrease at 0.6% H_2 in the desorption process. Based upon the

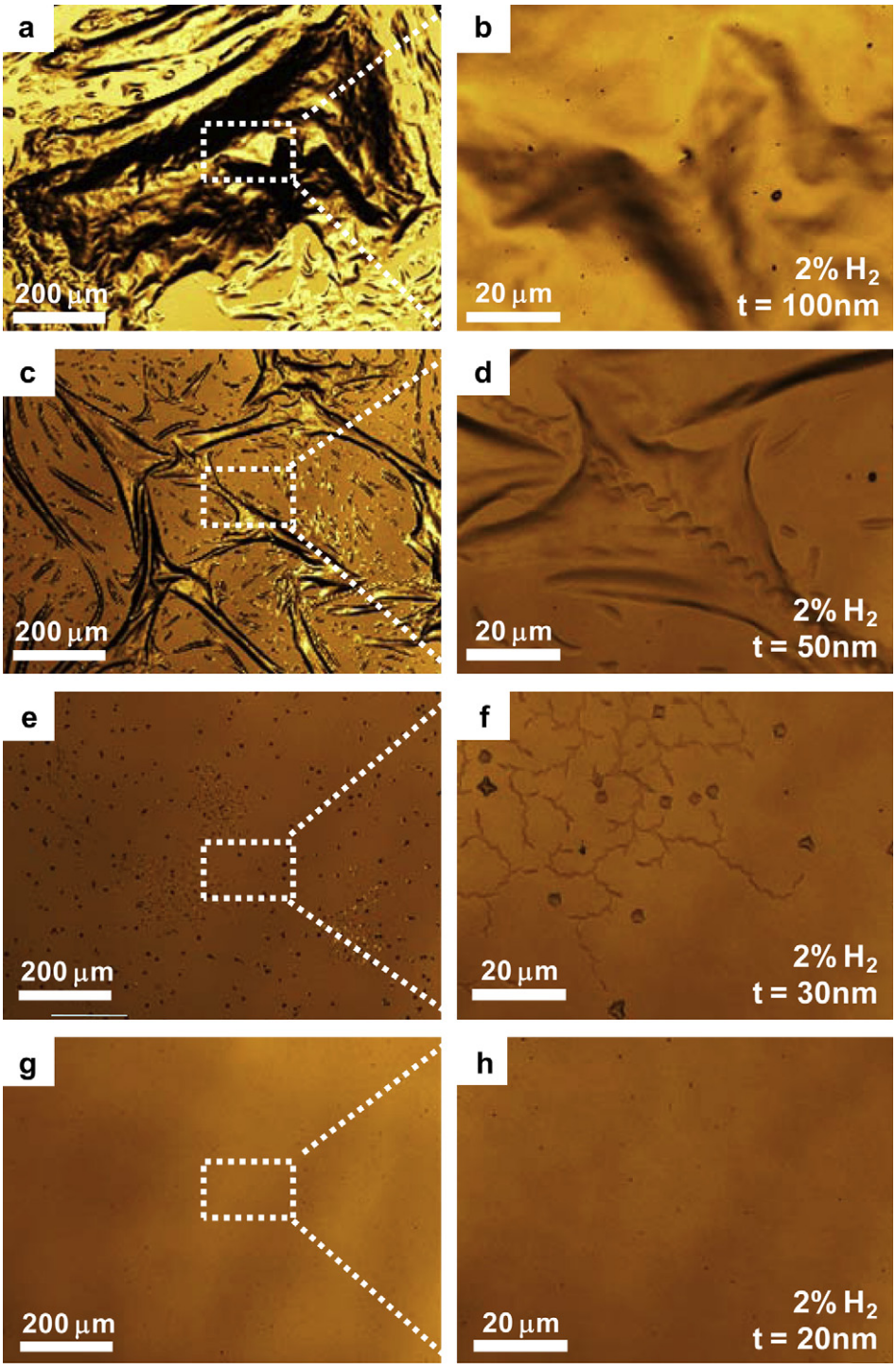

Fig. 3 – Scanning laser confocal images of the surfaces of the thin Pd films with different thicknesses of (a) 100 nm, (c) 50 nm, (e) 30 nm, and (g) 20 nm after the sample exposure to 2% H_2. Fig. 3(b), (d), (f) and (h) show the 10× magnified images of (a), (c), (e), and (g), respectively.

behavior of S, the Pd–H system can be divided into three different phases while varying the concentration of H_2. The first phase is the single α-phase (solid solution), and the α-phase remains until the concentration of H_2 is increased to 1.5% (S ≅ 12.1%), and this point is named as $p_{\alpha max/abs}$, which denotes the maximum partial pressure that α-phase can withstand during the absorption process. A gradual increase in S was observed up to $p_{\alpha max/abs}$, followed by a dramatic increase of S to 55% with increasing H_2 concentration to 1.7%. During the H_2 concentration intervals of 1.5–1.7%, both the α- and β-phases coexist, and thus this specific region of the graph was indicated as (α + β)-phase in Fig. 4(a). Owing to the

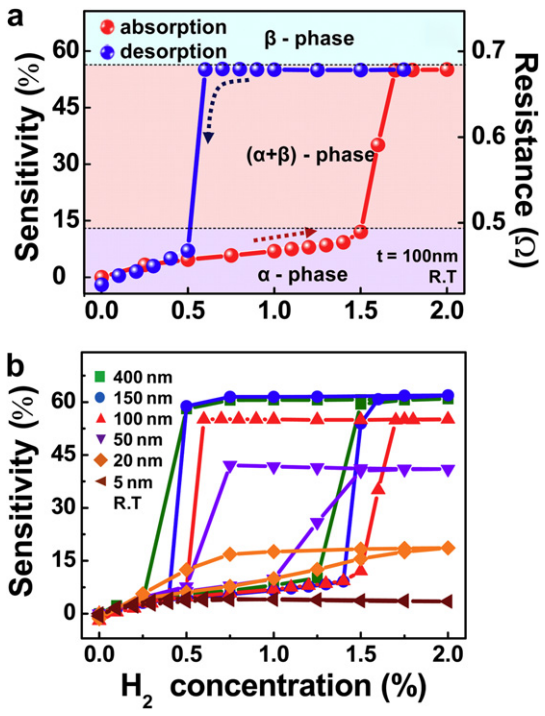

Fig. 4 – Hysteresis curve of sensitivity during the process of absorption and desorption of H by gradually changing the concentration of H_2 exposure from 0 to 2% (a) for the Pd thin film with thickness of 100 nm and (b) for the Pd thin film with different thicknesses ranging from 5 to 400 nm.

fact that both the α- and β-phases coexisted in the Pd thin film, S in this region depends on a composition ratio of the α- and β-phase, which can be described in the following equation [18]:

$$S = f_\alpha(S_{\alpha\ \max/\mathrm{abs}}) + f_\beta(S_{\beta\ \min/\mathrm{abs}}), \quad (2)$$

where f_α and f_β are the compositional fractions of the corresponding phases, and $S_{\alpha\max/\mathrm{abs}}$, $S_{\beta\max/\mathrm{abs}}$ are the sensitivities at $p_{\alpha\max}$ and $p_{\beta\min}$, respectively. Hence, it can be inferred that the large increase in S at this phase is primarily due to the formation of the β-phase, which is accompanied by the formation of defects such as vacancies and dislocations [20]. For the exposure of Pd film to H_2 concentrations greater than 1.7% during the absorption process, the phase was fully converted into a single β-phase (Pd–hydride), and S was saturated with further increase in H_2 concentration to 2%.

After the full phase transition of the Pd thin film to the single β-phase, the desorption process of H atoms was followed by reducing the concentration of H_2 back to 0%, and a hysteresis curve was obtained through the change in S. Notably, the maximum value of S remained nearly constant down to 0.6% H_2. It can be attributed to the stronger interaction force in the Pd–H bond of the single β-phase than that required to break the H–H bond in the formation of α-phase. During the H absorption process, H_2 molecules break into single H atoms in order to smear into the Pd layer and α-phase is generated. However, when transited to β-phase, H atoms have strong bonds with the Pd atoms and turning back to α-phase requires high activation energy to break these bonds. In other words, to break the bond between Pd and H atoms so that the H atoms can diffuse out of the Pd layer, the concentration gradient between the β-phase Pd:H film and the exposed environment should be sufficiently high enough to obtain the necessary driving force. As a result, the radical decrease of S is delayed to below 0.6% H_2 ambient during the desorption process.

Fig. 4(b) reveals the hysteretic behaviors of S when varying the exposure concentration of H_2 from 0 to 2% for Pd thin films with different thicknesses from 5 to 400 nm. The height of the hysteresis curve of S according to the varying thicknesses showed a clear tendency, where the difference between the values of S in the absorption/desorption processes increased linearly with respect to the thicknesses of the Pd film until 150 nm and saturated for further increase in the thickness. Accordingly, the effective region where the (α + β)-phase existed narrowed as the film thickness decreased [16]. The saturation of the sensitivity of Pd thin films with large thicknesses can be ascribed to the limit in the depth that H atoms can penetrate into the Pd layers, and thus phase transition can only occur near the surface of the thin film. In the course of the phase transition to β-phase, the octahedral sites of the Pd system are fully filled with H atoms, thereby expanding the lattice by approximately 10.9% in volume. However, as the film thickness decreases, the thin films are confined to the substrate tightly by the clamping effect, and hence further absorption of the H atoms and lattice expansion is restrained. This clamping effect increases as the thickness of the Pd thin films decreases. It was observed that for the Pd thin film of 5 nm thickness the hysteretic behavior vanished, meaning that the transition to the β-phase could also be restrained.

Fig. 5 exhibits the sensitivity of the Pd thin film in the α-phase during the absorption process. The sensitivity undergoes a gradual increase, which is in good agreement with the following Sieverts' law [13,23]:

$$S \propto \frac{H}{Pd} = \frac{1}{K_s}(pH_2)^{1/2}, \quad (3)$$

where H/Pd is the ratio of the atomic concentration of H to Pd in the Pd–H system (which is proportional to S), K_s is the Sieverts' constant, and pH_2 is the partial pressure of the H_2. It should be noted that in Fig. 5, the increase in the slope for different Pd film

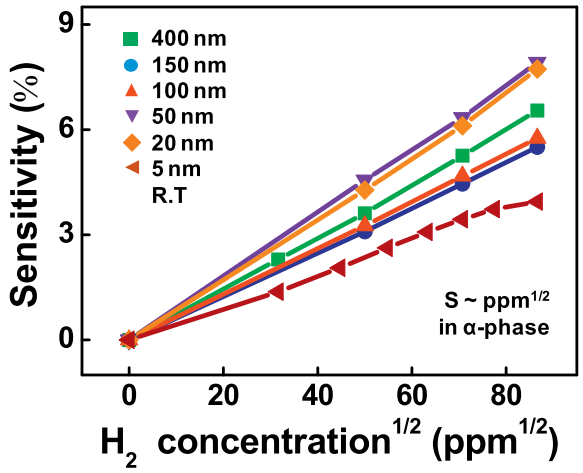

Fig. 5 – Change of sensitivity measured for α-phase Pd–H system in dilute H_2 ambient with different thicknesses from 5 to 400 nm during the H absorption process.

thicknesses was not accomplished with respect to linear changes in the film thickness, meaning that the values of K_s do not show any clear correlation with respect to the film thickness. Specifically, the values of K_s calculated for the film thicknesses of 5, 20, 50, 100, 150, 400 nm were 21.93, 11.31, 10.95, 15.13, 15.82, and 13.32, respectively. In the α-phase, two factors that determine the value of K_s are the effective exposed surface area of the Pd thin film and the penetration depth of H atoms into the Pd layer. Based on reiterated experimental results, we attribute the random behavior of the K_s values to the penetration depth of H atoms into the Pd layer, and believe that the optimized thickness of the film where a maximum amount of H atoms can be incorporated is approximately 50 nm. Hence, the highest sensitivity was achieved for 50 nm, followed by 20 nm, and then 400 nm.

4. Conclusions

The relationship between the change in R and the structural deformation of the thin Pd film due to the phase transition during the exposure to concentrated H_2 was extensively studied. According to the increase in the concentration of H_2, the phase of the Pd film made a transition into different phases from the initial α-phase: first to a coexisting phase of α- and β-phases, where an abrupt change in S was observed and to a complete β-phase where S saturated at approximately 55%. In the α-phase, the values of S increased in good accordance with the Sieverts' law. A remarkable hysteretic behavior of S was achieved during the absorption and desorption process of H atoms by controlling the environmental conditions of H_2 and N_2. The hysteretic behavior of S can be explained by the lower activation energy to break H–H bonding in the absorption process than that required for the breaking of Pd–H bond in the desorption process. The amount of variation in R, and thereby in S tends to minimize with decreasing thickness of the thin Pd film until the thickness reaches 5 nm for which the hysteretic behavior was terminated. The mechanical deformation of the thin Pd films corresponding to the transition of phases from α- to β-phase was effectively suppressed with decreasing film thicknesses. The present work reveals the effect of film thickness on the changes in the mechanical and electrical properties of pure Pd thin film-based sensors, which enables the fabrication of modified H_2 sensors that exhibit high sensitivity, fast response, and structural stability using pure Pd thin films.

Acknowledgments

This work was supported by the Agency for Defense Development through the Defense Nano Technology Application Center, Priority Research Centers Program (2009-0093823) through the National Research Foundation of Korea (NRF), the Basic Research Program grant (R01-2008-000-21078-0), Seoul Research and Business Development Program (10816). T Lee is grateful for the System IC 2010 program of the Ministry of Knowledge Economy, and Republic of Korea (10030517-2009-03, Advanced CMOS image sensor using 3D integration).

REFERENCES

[1] Bargthels H, Brocke WA, Bonhoff K, Julich P, Hydrogen Energy Prog. XI2; 1996.
[2] Agbossou K, Chahine R, Hamelin J, Laurencelle F, Anouar A, St-Arnaud JM, et al. Renewable energy systems based on hydrogen for remote applications. J Power Sources 2001;96:168–72.
[3] Goltsov VA, Veziroglu TN. A step on the road to hydrogen civilization. Int J Hydrogen Energy 2002;27:719–23.
[4] Firth JG, Jones A, Jones TA. The principles of the detection of flammable atmospheres by catalytic devices. Combust Flame 1973;21:303–11.
[5] Tabib-Azar M, Sutapun B, Petrick R, Kazemi A. Highly sensitive hydrogen sensors using palladium coated fiber optics with exposed cores and evanescent field interaction. Sens Actuators B 1999;56:158–63.
[6] Flanagan TB, Oates WA. The palladium–hydrogen system. Annu Rev Mater Sci 1991;21:269–304.
[7] Frazier GA, Glosser RJ. Characterization of thin films of the palladium–hydrogen system. Less-Common Met 1980;74:89–96.
[8] Shukla S, Seal S, Ludwig L, Parish C. Nanocrystalline indium oxide-doped tin oxide thin film as low temperature hydrogen sensor. Sens Actuators B 2004;97:256–65.
[9] Mor GK, Varghese OK, Grimes MA, Pishko MV. A room-temperature TiO_2-nanotube hydrogen sensor able to self-clean photoactively from environmental contamination. Mater Res Soc 2004;19:628–34.
[10] Lu G, Miura N, Yamazoe N. High temperature hydrogen sensor based on stabilized zirconia and a metal oxide electrode. Sens Actuators B 1996;35–36:130–5.
[11] Graham T. On the absorption and dialytic separation of gases by colloid septa. Philos Trans R Soc 1866;156:399–439.
[12] Lewis FA. The palladium hydrogen system. Academic Press; 1967.
[13] Cabrera AL, Aguayo-Soto R. Hydrogen absorption in palladium films sensed by changes in their resistivity. Catal Lett 1997;45:79–83.
[14] Xu T, Zach MP, Xiao ZL, Rosenmann D, Welp U, Kwok WK, et al. Self-assembled monolayer-enhanced hydrogen sensing with ultrathin palladium films. Appl Phys Lett 2005;86:203104.
[15] Katsuki A, Fukui K. H_2 selective gas sensor based on SnO_2. Sens Actuators B 1998;52:30–7.
[16] Kang BS, Ren F, Gila BP, Abernathy CR, Pearton S. AlGaN/GaN-based metal–oxide–semiconductor diode-based hydrogen gas sensor. J Appl Phys Lett 2004;84:1123.
[17] Lundstrom I, Shivaraman S, Svensson C. A hydrogen sensitive Pd-gate MOS transistor. J Appl Phys 1975;46:3876–81.
[18] Sakamoto Y, Takashima I. Hysteresis behaviour of electrical resistance of the Pd–H system measured by a gas-phase method. J Phys Condens Matter 1996;8:10511–20.
[19] Tsukahara M, Takahashi K, Mishima T, Isomura A, Sakai T. Influence of various additives in vanadium-based alloys $V_3TiNi_{0.56}$ on secondary phase formation, hydrogen storage properties and electrode properties. J Alloys Compd 1996;245:59–65.
[20] Chtanov A, Gal M. Differential optical detection of hydrogen gas in the atmosphere. Sens Actuators B 2001;79:196–9.
[21] Fedtke P, Wienecke M, Bunescu MC, Pietzak M, Deistung K, Borchardt E. Hydrogen sensor based on optical and electrical switching. Sens Actuators B 2004;100:151–7.

[22] Jeon KJ, Jeun MH, Lee E, Lee JM, Lee K, Allmen P, et al. Finite size effect on hydrogen gas sensing performance in single Pd nanowires. Nanotechnology 2008;19:495501.
[23] Hughes RC, Schubert WK, Buss R. Solid-state hydrogen sensors using palladium-nickel alloys: effect of alloy composition on sensor response. J Electrochem Soc 1995;142:249–54.
[24] Hughes RC, Schubert WK, Zipperian TE, Rodriguez JL, Plut TA. Thin-film palladium and silver alloys and layers for metal-insulator-semiconductor sensors. J Appl Phys 1987;62: 1074–83.
[25] Othonos A, Kalli K, Tsai DP. Optically thin palladium films on silicon-based substrates and nanostructure formation: effects of hydrogen. Appl Surf Sci 2000;161:54–60.
[26] Dus R, Nowakowski R, Nowicka E. Chemical and structural components of work function changes in the process of palladium hydride formation within thin Pd film. J Alloys Compd 2005;404–406:284–7.
[27] Goltsova MV, Artemenko YA, Zaitsev VI. Kinetics and morphology of the reverse $\beta \rightarrow \alpha$ hydride transformation in thermodynamically open Pd–H system. J Alloys Compd 1999; 293–295:379–84.
[28] Hughes RC, Schubert WK. Thin films of Pd/Ni alloys for detection of high hydrogen concentration. J Appl Phys 1992; 71:542–4.
[29] Kibria AKMF, Sakamoto Y. Hysteresis of pressure-composition and electrical resistance-composition isotherms of palladium–silver alloys–hydrogen system. Mater Sci Eng B 1998;53:256–61.
[30] Luongo K, Sine A, Bhansali S. Development of a highly sensitive porous Si-based hydrogen sensor using Pd nano-structures. Sens Actuators B 2005;111:125–9.
[31] Kumar MK, Rao MSR, Ramaprabhu S. Structural, morphological and hydrogen sensing studies on pulsed laser deposited nanostructured palladium thin films. J Phys D Appl Phys 2006;39(13):2791.
[32] Elam JW, Zinovev A, Han CY, Wang HH, Welp U, Hryn JN, et al. Atomic layer deposition of palladium films on Al_2O_3 surfaces. Thin Solid Films 2006;515:1664–73.
[33] Ding D, Chen Z, Lu C. Hydrogen sensing of nanoporous palladium films supported by anodic aluminum oxides. Sens Actuators B 2006;120:182–6.
[34] Rahimi F, zad AI, Razi F. Palladium plating on macroporous/ microporous silicon: application as a hydrogen sensor. Synthesis and reactivity in inorganic, Metal; 2007;37:p. 377–80.
[35] Penza M, Cassano G, Tortorella F. Gas recognition by activated WO_3 thin-film sensors array. Sens Actuators B 2001;81:115–21.
[36] Mitra P, Chatterjee AP, Maiti HS. ZnO thin film sensor. Mater Lett 1998;35:33–8.
[37] Varghese OK, Gong D, Paulose M, Ong KG, Grimes CA. Hydrogen sensing using titania nanotubes. Sens Actuators B 2003;93:338–44.